DESIGN AND CONFIGURATION LAYOUTS OF AN ADVANCED LONG ENDURANCE UAV- LESSONS LEARNT AFTER FLIGHT TESTING

Zdobyslaw Goraj, Miroslaw Rodzewicz, Wojciech Grendysa, Marek Jonas
Warsaw University of Technology
goraj@meil.pw.edu.pl;miro@meil.pw.edu.pl

Keywords: *UAS, aircraft design, stability, trimming*

Abstract

This paper is focused on design, optimisation, dynamic research and testing of UAV system for long endurance border surveillance having high-level requirements in term of reliability, safety and low cost. Comparisons between 3 configurations – one tailed and 2 tailless - based on flight experience, are analysed to show expected advantages and possible drawbacks. A special attention was devoted to trimming, stability, control and take-off of tailless configuration. After a theoretical analysis and optimisation a number of free flight tests were performed and most of numerical predictions and theoretically prepared procedures were fully confirmed.

1 General Introduction

SAMONIT is an acronym of a national Polish project, financially supported by Ministry of Science and Higher Education. The main goal of the activity within this project was to design an UAV system for long endurance border surveillance and monitoring having high level requirements in term of reliability and safety and being affordable for potential users in terms of cost [1-5]. The design process was treated as an interdisciplinary approach, and included a selection of thick laminar wing section, aerodynamic optimisation of swept wing, stability analysis, weight balance, structural and flutter analysis, many on-board redundant systems, reliability and maintainability analysis, safety improvement, cost and performance optimisation [6-8]. It was developed by a group researchers and designers having a very wide experience gained in various former projects, both industrial and academic and also involved in many international, mainly European V, VI and VII FP projects [9-10].

2 Design and configurations

This paper is focused on design, optimisation, dynamic research and testing of a mini UAS called SAMONIT [11-17]. A baseline configuration (straight wing with V-tailplane placed behind the main wing) is used as a reference for more advanced layouts, especially swept tailless configuration, considered as the goal configuration in two versions – with pulling and pushing propellers. Comparisons between these 3 configurations based on free flight experience, are analysed to show expected advantages and possible drawbacks. Flight-testing has been started in the fall of 2009 and it is still in progress, both in manual and automated modes. All 3 prototype airplanes flew more than 10 hours [18-19] and delivered a lot of interested data of high importance for performance, safety, flight control, maintenance, flight preparation time, repair after small damages, sensitivity to weather conditions etc. Figures and photos attached bellow (Fig. 1-8) show some important details and phases of the project.

3 Trimming, control and stability

Trimming, control and stability were analysed through the whole time of the project since its

kick-off. A special attention was devoted to flying wing configurations. Team of designers were conscious that successful solution of challenges of stability and controllability can decide about the dynamic properties of the vehicle and either a success or failure of the project. Advantages, drawbacks and risk associated with tailless configuration are well known for decades. Selected problems must be treated with special care. These include optimal centre gravity location for proper static stability margin, limitation of flaperons' hinge moments, ensuring that the flaperons and rudders are efficient and robust in regular flights and in hazardous states (for example if one engine failed), achieving the dynamically stable platform and many others. In aviation history there were not too many very successful tailless aircraft. VeryEasy designed by Burt Rutan and B2 by Northrop Grumman are rather exceptions among manned airplanes, also the KillerBee by Swift Engineering among unmanned versions are good examples of successful designs. However, it is very difficult to find in open sources any aerodynamic characteristics of tailless aircraft, their stability derivatives, times to double and similar dynamic properties. So, when working on SAMONIT, one had to analyze the stability and manoeuvrability in the so-called full cycle, i.e. since conceptual project, through Wind Tunnel tests till free flight tests. During the critical design review, organized after the number of flight tests, the final configuration was approved and accepted as the test-bad for more advanced free flight testing.

All numerical analyses were based on aerodynamic characteristics and static stability derivatives measured for full scale platform in a large wind tunnel Φ5 at the Institute of Aviation. The so-called dynamic stability derivatives (lp, l_r, n_p, n_r,) were computed using CFD software and also assessed using ESDU sheets. Trim parameters and stability characteristics are shown at figures 9-30 and discussed below. At Fig.70 trim parameters – i.e. thrust required for steady horizontal flight, angle of attack and flaperons deflection – all versus flight speed - are presented. These results were computed for aircraft weight equal to 48 kg, centre of gravity located at 8% of MAC, what means that for neutral point of static stability located at 29% of MAC and measured from MAC LE it gives the stability margin equal to 21% of MAC. At Fig. 9 two characteristic speeds are distinguished – stall speed corresponding to $C_{L,max}$=1.4 for clean configuration and max speed corresponding to the maximum available power equal to 10,5 horsepowers. Stall speed and maximum speed are equal to 21 m/s (75 km/h) and 48 m/s (172 km/h), respectively. Curves of required thrust, angle of attach and flaperons deflection are typical. A possible correction might include a vertical shift of the flaperons deflection curve in order to ensure the flaperon deflection corresponding to loiter speed is equal to zero (what means that loiter speed gives the best aerodynamic efficiency and the minimum fuel consumption). This effect could be achieved by redesign of the wing, however it is not planed at this stage of the project.

Fig. 10 shows the damping and frequency coefficients for Short Period mode. Increasing the speed results in better damping and makes the mode stiffer, i.e. increases its frequency. The change of damping coefficient and frequency versus flight speed is rather typical for Short Period mode – the mode is strongly damped and its frequency increases from $f = 1/T = 1/(2\pi/\eta) = 1/1{,}9 = 0.52$ Hz at lower speeds to about 0,87 Hz at higher speeds.

Fig. 11 shows the damping and frequency coefficients for Phugoid mode. A slight instability can be observed at small flight speed and then stability if flight speed is greater than 26 m/s. Time to double (what is a measure of instability) is greater than 17 s ($T2 = -\ln 2/\xi = -0.69/0.05 = -17.25$) and can be accepted without reservations because it is longer than the expected time of transition through the range of small speeds. Frequency of oscillation changes from $f = 1/T = \eta/2\pi = 0.58/2\pi = 0.09$ Hz at small flight speed to 0.039 Hz at higher speeds.

Fig. 12 shows the damping and frequency coefficients for Dutch Roll mode. Dutch Roll is well damped at the whole range of flight speed and time to half is $T_{1/2}$ = 3.39 s. Frequency of oscillation changes from f = 1/T =

$\eta/2\pi = 2/2\pi =$ 0.32 Hz at small flight speeds to about 0.79 Hz at high flight speeds.

Fig. 13 presents damping coefficients for Spiral mode versus flight speed computed for effective dihedral angle equal to 2^o. The so-called "design dihedral" is equal to -2^o, and the "effective dihedral" is equal to $+2^o$, what follows from wing deflection due to external load. Minimum time to double is T_2= 10.5 s, what is sufficient for transition through range of small speeds during take-off and landing.

Fig 14 shows damping coefficients for Spiral mode if effective dihedral angle is much higher ($\Gamma = +10^o$). It is rather a theoretical case, not to be fulfilled in real design. The corresponding minimal time to double T_2= 17.5 s. This result clearly shows that a very essential design change does practically not influence on Spiral damping and therefore should not be considered at all.

Damping and frequency coefficients for Dutch Roll mode are presented in Fig. 15-16. In both cases Dutch Roll is stable and an influence of dihedral angle on the rate of damping can be seen at higher flight speeds but still it is not an essential. For the contrary, area of winglets plays important role in Dutch Roll stability. Increasing of winglets from S_v = 0.132 m^2 to 0.210 m^2 (it is the area of both winglets on left and right wing) accelerates the Dutch Roll damping and also increases its frequency. However, the Dutch Roll is sufficiently damped even with smaller winglets and therefore there is no need for increase of winglets area.

An influence of winglet area on damping of Spiral mode is shown at Fig. 17. Increase of winglets area decreases time to double and therefore it is not recommended. So, designers decided not to increase the winglets, even that they can improve the damping of Dutch Roll.

At Fig. 18 there are shown 2 analytical drag polars – a real drag polar (measured in wind tunnel) and a virtual drag polar (taken for Phugoid stability analysis). Fig. 19 presents damping coefficients of Phugoid computed compared for both drag polars. It can be seen that the so-called "flat drag polar" (small drag coefficient in a wide range of lift coefficient – see real drag polar in Fig. 18) gives a slightly unstable Phugoid at small flight speed, and for the contrary the so-called "steep drag polar" (small drag coefficient at lower lift coefficients and higher drag coefficients at higher lift coefficients) leads to stable Phugoid also at small flight speeds. This observation does not mean that one can deteriorate drag polar to get a stable Phugoid, but explains why in some cases the Phugoid is unstable. This instability occurs at small flight speeds and can be easily improved by autopilot or manual pilot in the Ground Control Station. Frequency coefficient shown at Fig. 20 does not depend practically on the shape of polar drag.

Fig. 21 presents the stability of Short Period and Phugoid modes versus the centre of gravity position, x_C. For x_C greater than 23% of MAC (measured from leading edge (LE) of MAC) both modes are strongly coupled and unstable. Basing on the Fig. 21 it is possible to determine the rear position of the x_C. Coming from the assumption that a static stability margin is equal to 5% of MAC it can be established that the rear position of the x_C should not be greater than 20% of MAC. This value can be slightly changed for different flight speed, flight altitude, mass of aircraft (see Fig. 23).

Fig. 22 presents the influence of the centre of gravity position, x_C on flaperons deflection for aircraft trimming. This figure can deliver an information about the forward limit of the centre of gravity position, what follows from the maximum flaperons deflection. Moreover, the large value of flaperons deflection for trimming is associated with the aerodynamic drag increase and results in range and endurance decreasing.

Fig. 23-24 present results for flight speed equal to 40 m/s and are equivalent to Fig. 21-22 corresponding to flight speed equal to 22 m/s. It follows from Fig. 23 that the limit rear centre of gravity position must be shifted forward to about 18% and moreover that for higher flight speeds the forward limit of the centre of gravity position is not bounded by a high flaperons deflection for trimming.

Fig. 25 shows deflection of rudder required for a steady horizontal flight trimming in case when one engine is not operated (only right engine is working). Curves of rudder

deflections are not continuous what follows from the fact that the software STB is not well suited for asymmetric power unit. Due to a luck of data on yawing moment generated by asymmetric power unit it was decided to compute the trim conditions under the assumption that yawing moment is constant in a number of speed ranges. From Fig. 25 it follows that the flight at small speeds generates a critical case, because the rudder deflection required for trimming of steady horizontal flight without sideslip is equal to -25^o (i.e. too much). One can get a simpler solution if the sideslip is allowed. It must be noticed that positive and negative sideslips require a mutual symmetric deflections of flaperons and rudder, see Fig. 26.

Flight in sideslip with one engine dead make it possible to chose a flight configuration. If one assume that the working engine is located on the right side of the aircraft, it would be possible to keep the failed engine on the lee side. In such a case the aircraft will fly with positive sideslip and the rudder deflection for trimming would be equal to 35^o what is unrealistic. However, if one keep the failed engine on the windward side, it means that the sideslip is negative and rudder deflection would be -12^o only what is fully realistic, see Fig. 27. These possible flight configurations for positive and negative sideslip are shown at Fig. 28.

Fig. 29 presents range and endurance of the platform (tailless tractor configuration) with a fixed-pitch propeller at its maximum efficiency = 0.8. At See Level flight altitude the specific fuel consumption was measured both in laboratory and in flight and is equal to $SFC=3.388 * 10^{-6}$ [1/m]. For computation it was assumed basing on wind tunnel results that $C_L=0.5$; $C_D=0.034$; $C_L/C_D=14.4$; $C_L^{3/2}/C_D=10.39$. For aircraft weights - initial $m_0=60$ kg and final $m_K=36$ kg - the endurance was 12 h. For initial weight $m_0=88$ kg and final weight $m_K=54$ kg the endurance would be E=18.8 h.

Fig. 30 shows trim parameters at take-off run. Green colour is used to mark a margin for a safe take-off. Such the safe take-off should be performed at the speed for lifts of the ground V=24 m/s (or higher) and flaperons deflected on -4^o. Decreasing the speed for lifts of the ground bellow V=24 m/s would result in deflection of flaperons up to -5^o and entering into the range of speeds lower than $1.2*V_{STALL}$ for $\delta_H=0^o$, i.e. decreasing a safe margin of speed between V_{STALL} and V_{MIN}. The absolute V_{MIN} during take-off for the configuration corresponding to m=51 kg and $x_C=14\%$ is equal V=23 m/s, because at this speed there is no risk to have too small speed margin even at $\delta_H=-20^o$. Red colour at Fig. 30 marks the boundary of the safe speed margin (assuming that angles of attack are equal to those computed from trim conditions and are not exceeded) and the pink colour marks the boundary of the safe speed margin (assuming that angles of attack could be greater than those computed from trim conditions and could reach even to 20^o). Blue colour is used to mark the trim conditions (α,δ_H) versus flight speed for the so-called changeable configuration (i.e. δ_H deflected according to trim conditions). Red stars correspond to the take-off rotational speed at $\alpha = 3^o$, for different flaperons deflections $\delta_H = -20^o, -4^o, 0^o, -20^o$, from the left star to the right star, respectively.

4 Conclusions

The most important conclusions could be summarised as follows:
(1) V-tail enables a relatively easy parachute deployment in emergency with a minimal risk of getting into propeller. However, longitudinal and lateral control is coupled what can involve difficulties, especially at higher angles of attacks; (2) V-tail configuration with 2 isolated, laterally shifted segments decreases its anti-spin characteristics; (3) Take-off minimum speed for tailless configuration is higher than for the classical one. Moreover, control during take-off must be more precise for tailless configuration than for the tailed one because flaperons deflection influence both on pitching moment and lift. If trailing edges of flaperons go up, then pitching moments increase and lift decrease what can result in airplane stall if the airplane speed is too small. In the case of tailed configuration the lift and pitching moment are controlled independently – lift by flaps and pitching moment by elevator deflections; (4)

Tailless configuration offers much higher maximum flight speed and the so-called "wetted aspect ratio". So, for the long endurance missions this configuration offers better performance; (5) Tailless pushing configuration has even higher maximum speed than the corresponding tractor configuration. It is because of wider area of natural laminar flow over the wing in the neighbourhood propellers and nacelles. The corresponding maximum speeds achieved during flight tests were 39 m/s, 45 m/s and 53 m/s for tailed, tailless tractor and tailless pushing configuration, respectively; (6) Rudders located on winglets in tailless tractor configuration are effective in most of manoeuvres. However, if one engine is inoperative the rudders are too small for trimming. Pushing configuration with rudder located on vertical tail attached to the central container is fully effective irrespectively on flight regime; (7) Both tailless configurations offer better access to all on-board systems and sensors. Also, time of assembling and de-assembling is shorter in the case of flying wing configuration.

5 Design details and numerical results

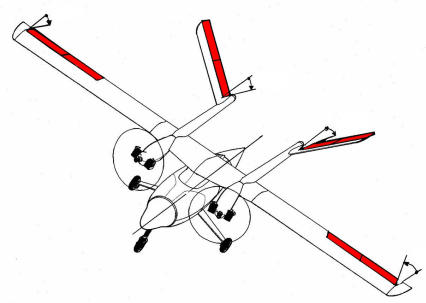

Fig. 1 SAMONIT in classical, tailed, tractor configuration. Flight control surfaces are marked in red colour

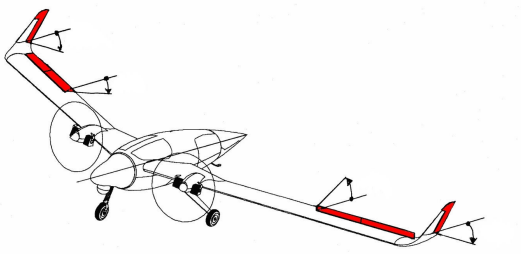

Fig. 2 SAMONIT in tailless, tractor configuration. Flight control surfaces are marked in red colour

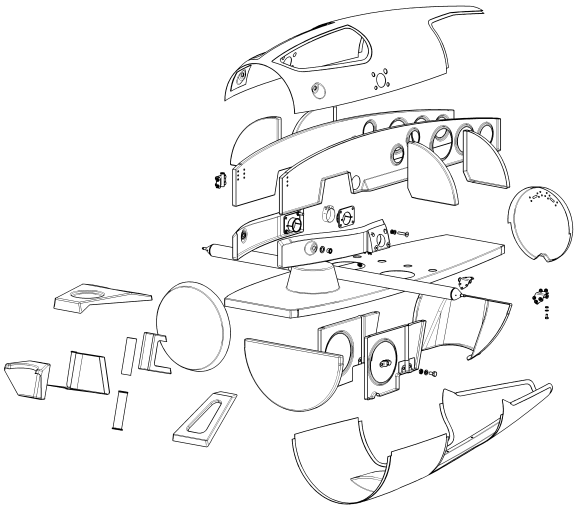

Fig. 3. Structure of the container for main on-board systems and sensors

Fig. 4 SAMONIT in tailless configuration with pushing propellers

Fig. 5 Airplane in tailed, tractor configuration. Flight test with autopilot in the loop. Daylight camera (FLIR) visible at the nose of the container. Sochaczew, April 2011.

Fig. 6 Airplane in tailless, tractor configuration. Flight test in manual mode. Daylight camera visible at the nose of the container. Sochaczew, September 2010.

Fig. 7 Ground preparation for flight-testing. Tailless, pushing propeller airplane on the left, the classical V-tail configuration on the right and Ground Control Station (also used for transport of airplane parts) behind. Minsk Mazowiecki, July 2011.

Fig. 8 Tailless, pushing propeller airplane after flight show, just before touchdown. Minsk Mazowiecki, July 2011.

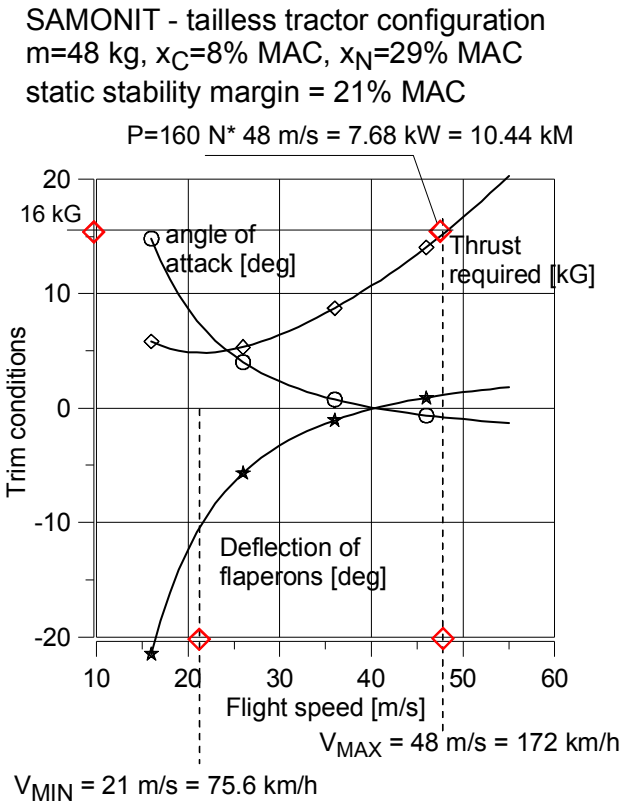

Fig. 9 Parameters in trim – thrust required, angle of attack and flaperons deflections

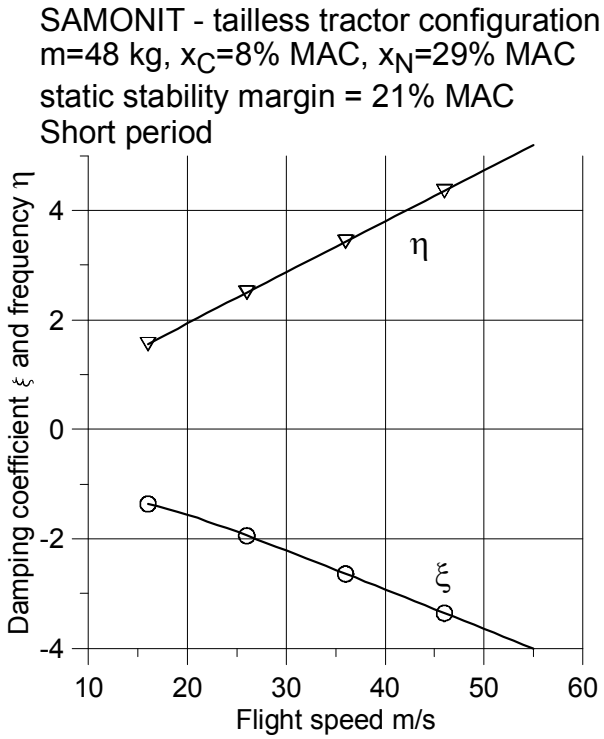

Fig. 10 Damping coefficients and frequencies for Short Period mode versus flight speed

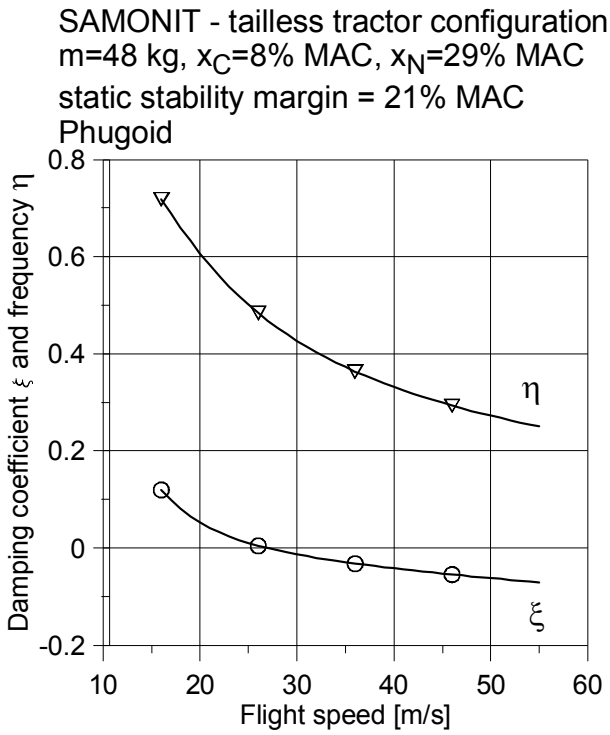

Fig. 11 Damping coefficients and frequencies for Phugoid mode versus flight speed

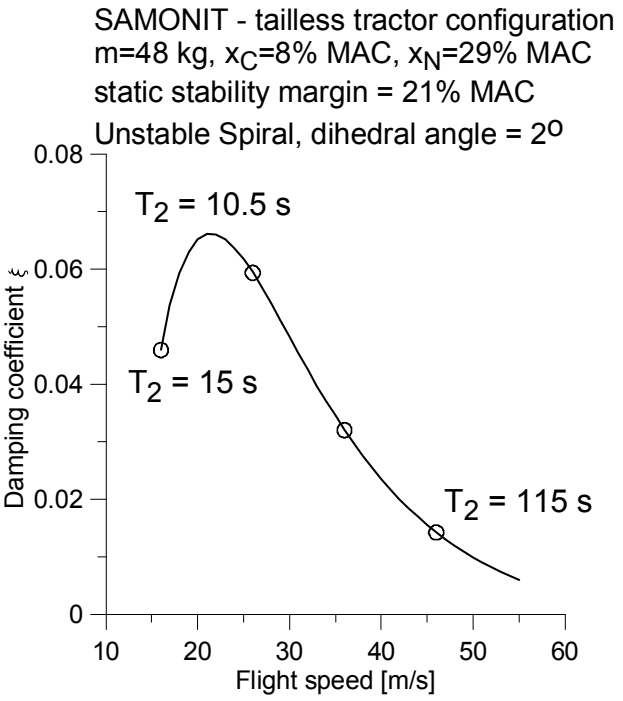

Fig. 13 Damping coefficients for Spiral mode versus flight speed, dihedral angle equal to 2°

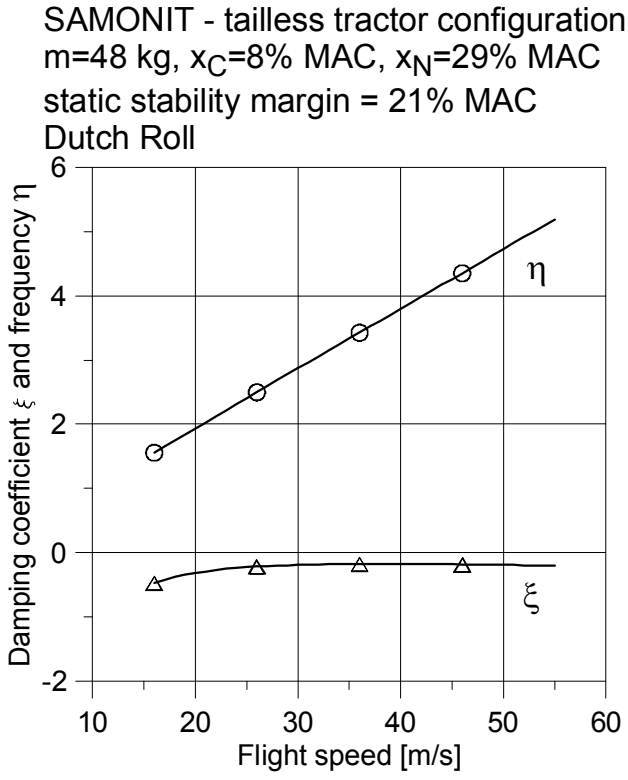

Fig. 12 Damping coefficients and frequencies for Dutch Roll mode versus flight speed

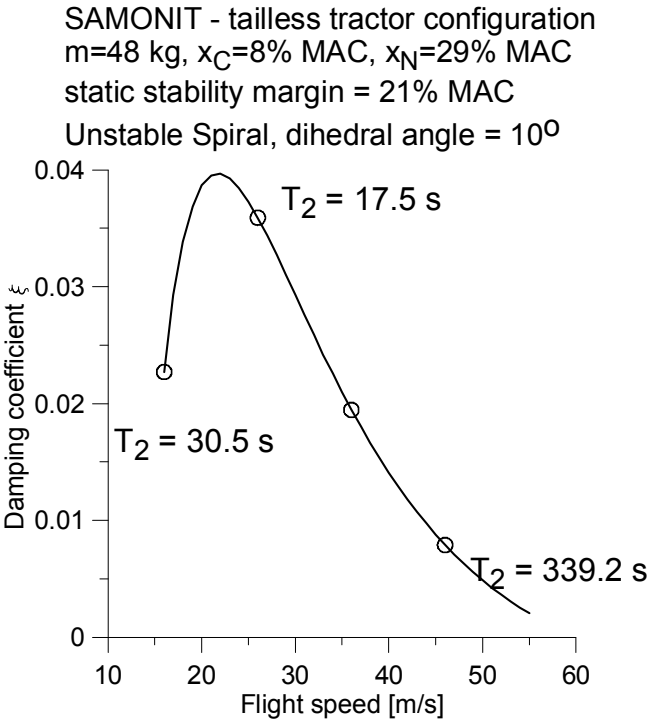

Fig. 14 Damping coefficients for Spiral mode versus flight speed, increased dihedral angle equal to 10°

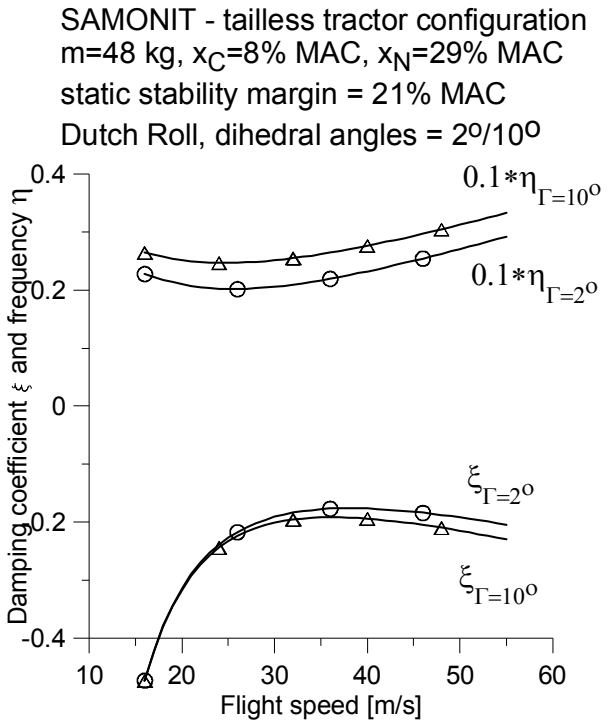

Fig. 15 Damping coefficients and frequencies for Dutch Roll mode versus flight speed – comparison between different dihedral angles - 2° and 10°

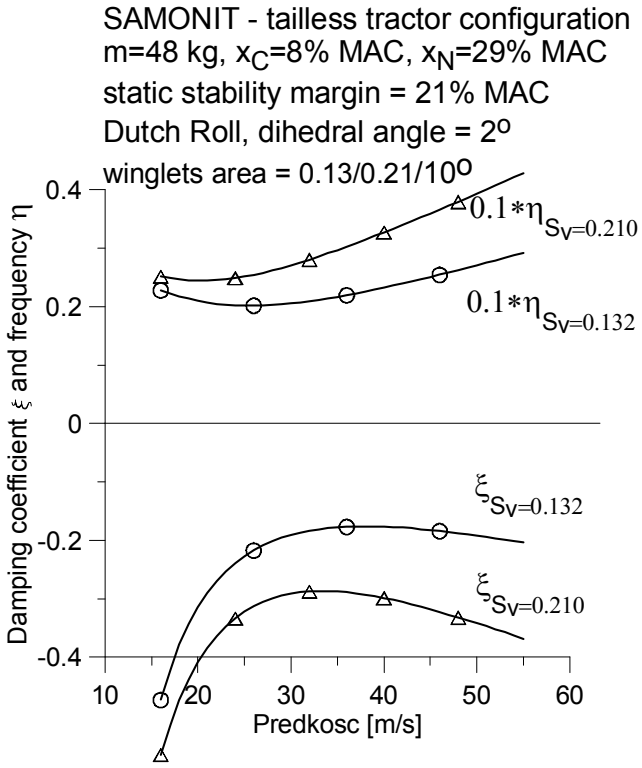

Fig. 16 Damping coefficients and frequencies for Dutch Roll mode versus flight speed – comparison between different areas of vertical stabilizer – S_V =0.132 m^2 and S_V =0.210 m^2

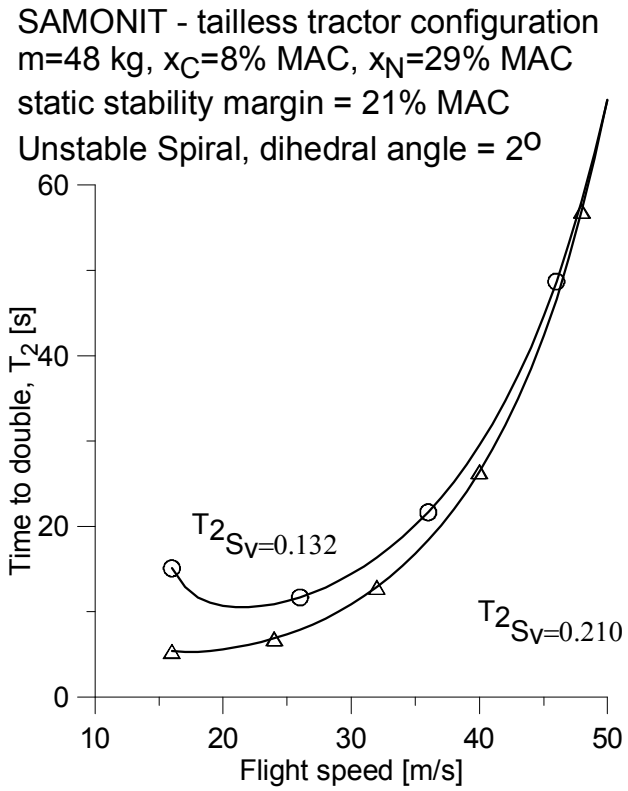

Fig. 17 Damping coefficients for Spiral mode versus flight speed – comparison between different areas of vertical stabilizer – S_V =0.132 m^2 and S_V =0.210 m^2

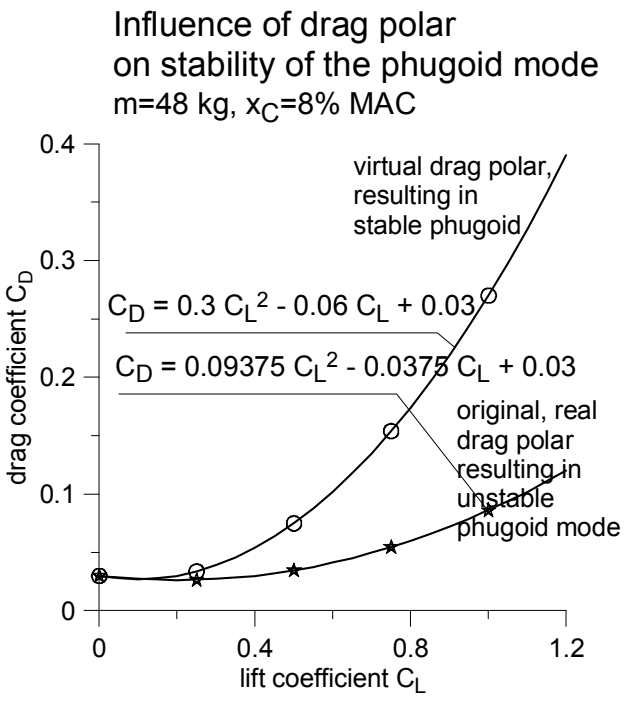

Fig. 18 Drag polars of SAMONIT tailless tractor configuration - original, real drag polar resulting in unstable Phugoid mode and a virtual drag polar leading to stable Phugoid mode

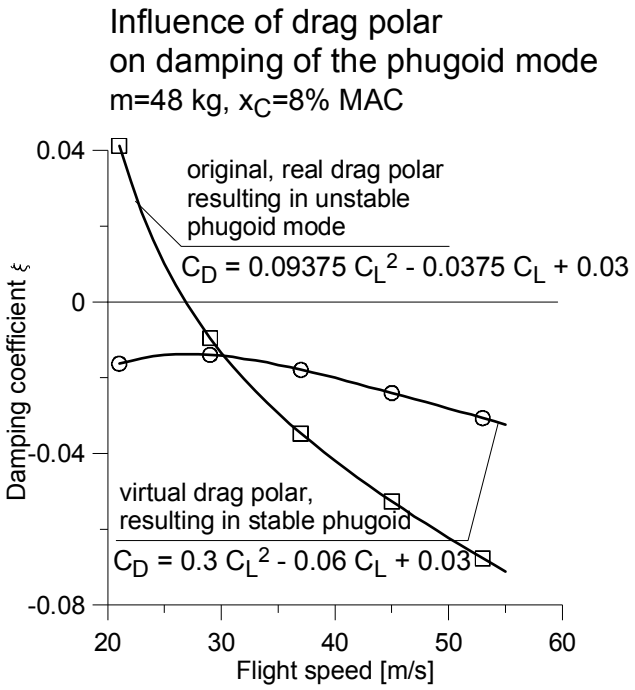

Fig. 19 Damping coefficients for Phugoid mode – obtained for original, real drag polar resulting in instability and a virtual drag polar leading to stable mode

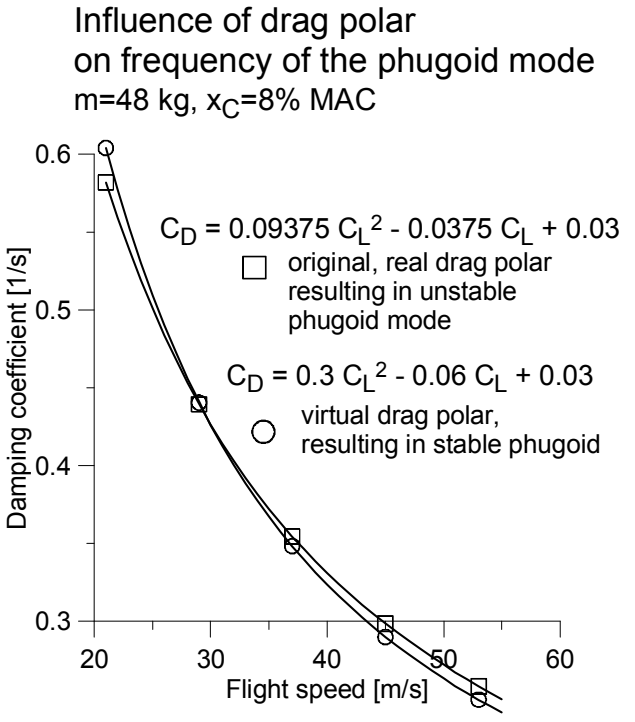

Fig. 20 Frequencies of Phugoid mode do not practically depend on the shape of drag polar

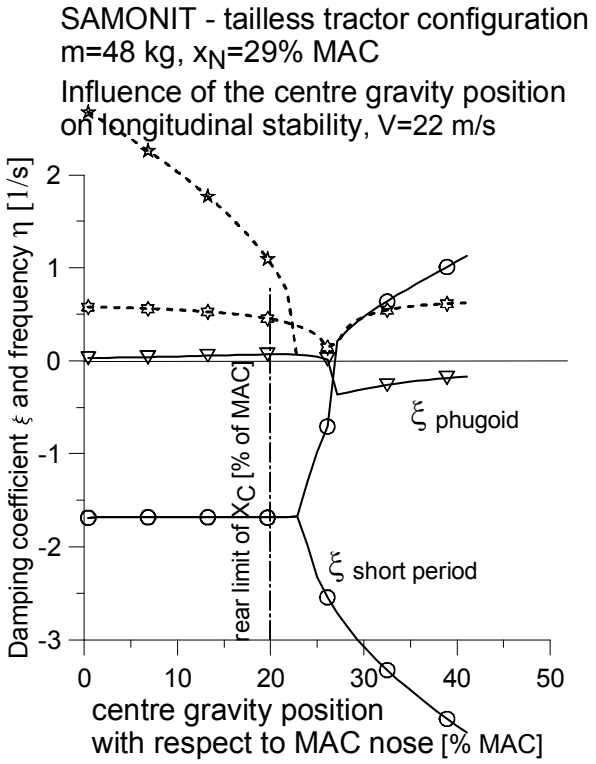

Fig. 21 Influence of the centre gravity position on Phugoid and Short Period stability, for flight speed V=22 m/s

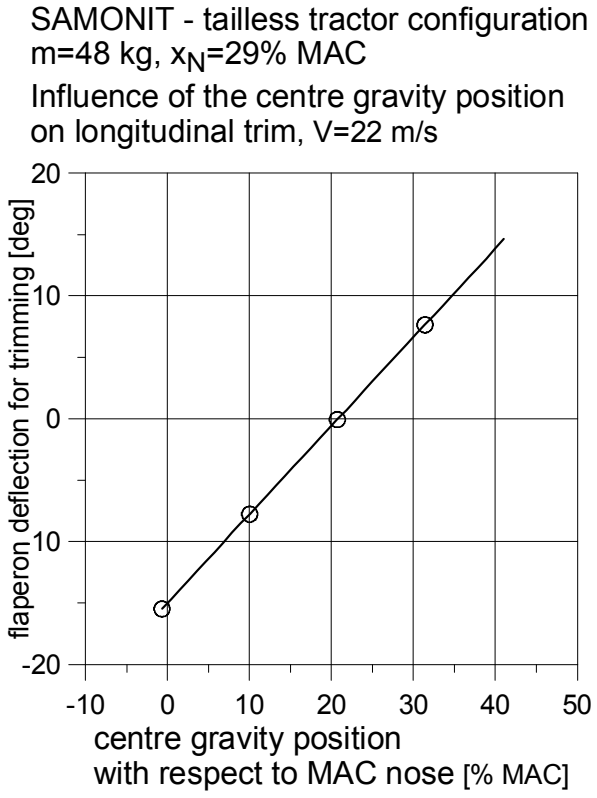

Fig. 22 Deflection of flaperons for trimming versus the centre gravity position, for flight speed V=22 m/s

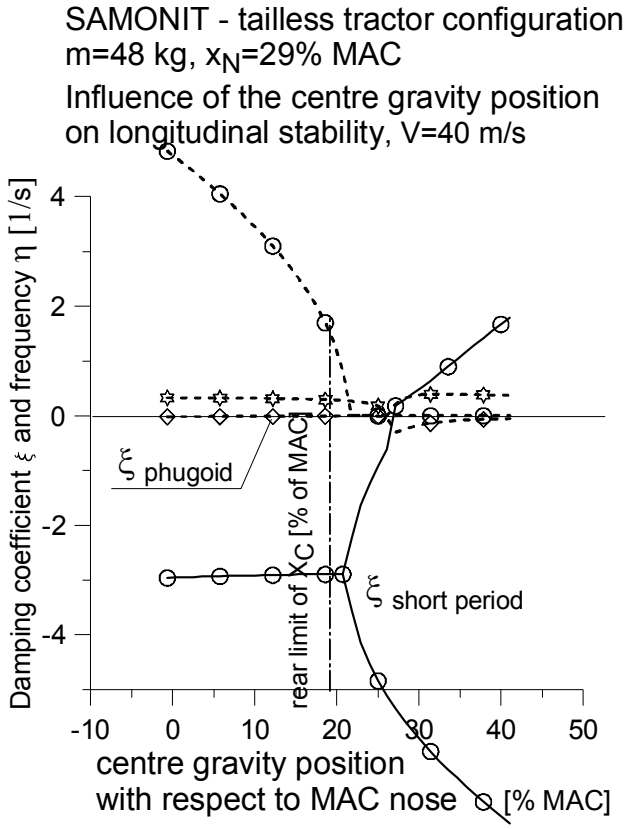

Fig. 23 Influence of the centre gravity position on Phugoid and Short Period stability, for flight speed V=40 m/s

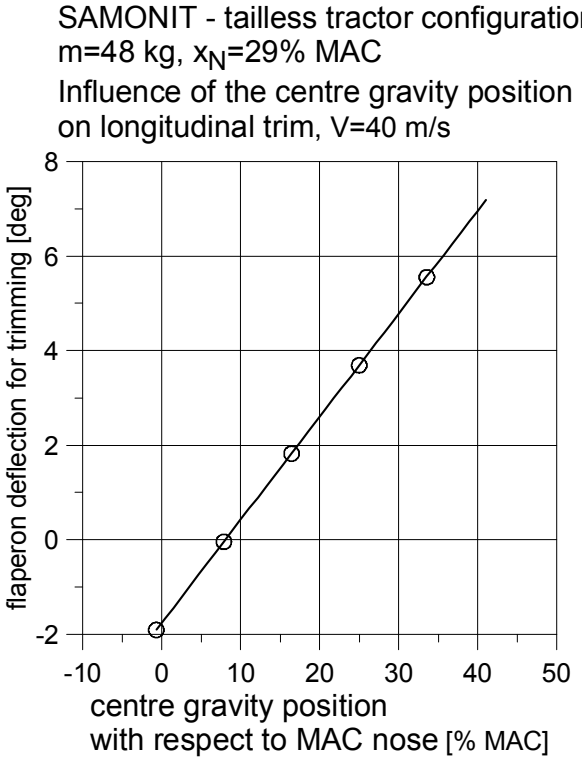

Fig. 24 Deflection of flaperons for trimming versus the centre gravity position, for flight speed V=40 m/s

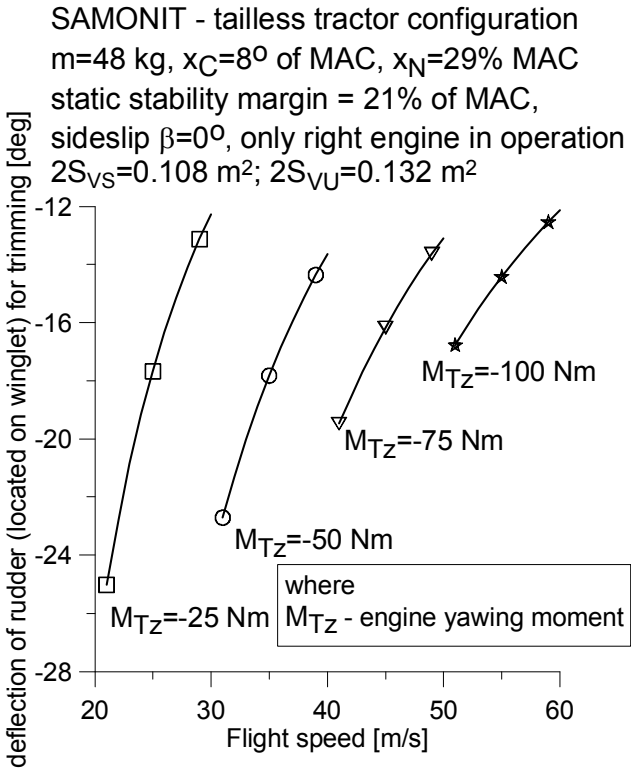

Fig. 25 Deflection of rudder for trimming versus flight speed at hazardous state, one engine not operated

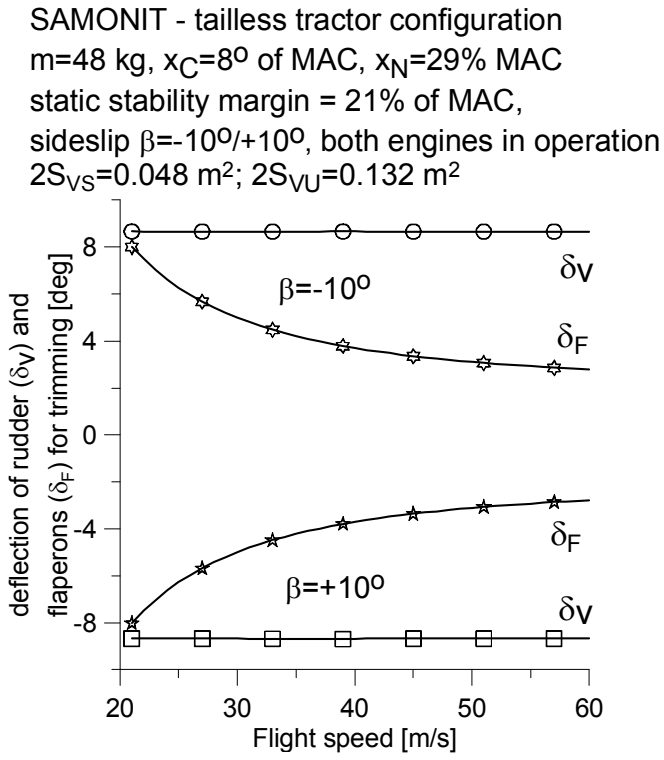

Fig. 26 Deflection of flaperons and rudder for trimming versus flight speed at sideslips

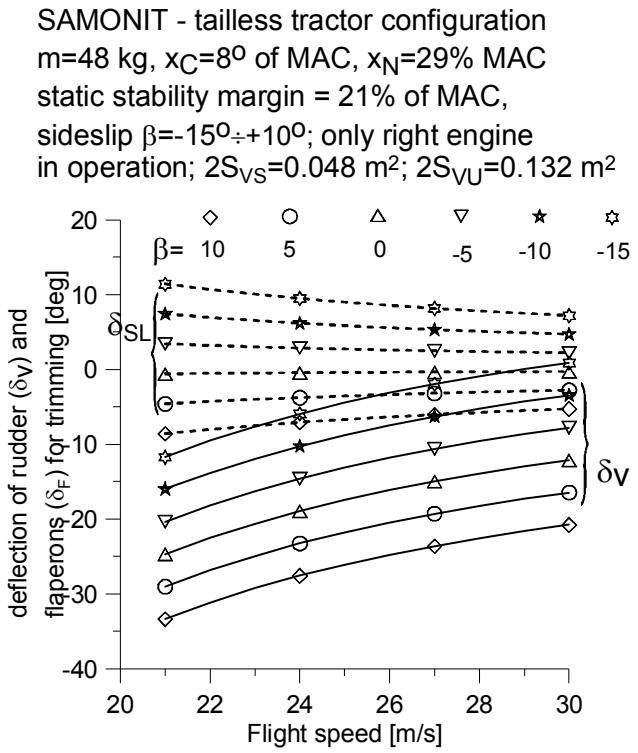

Fig. 27 Deflection of flaperons and rudder for trimming versus flight speed at different sideslips, only right engine in operation

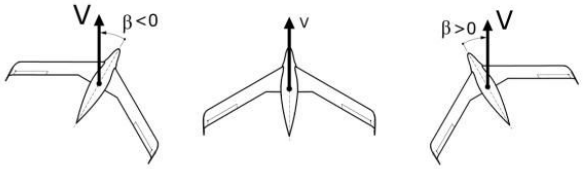

Fig. 28 Definition of positive and negative sideslips

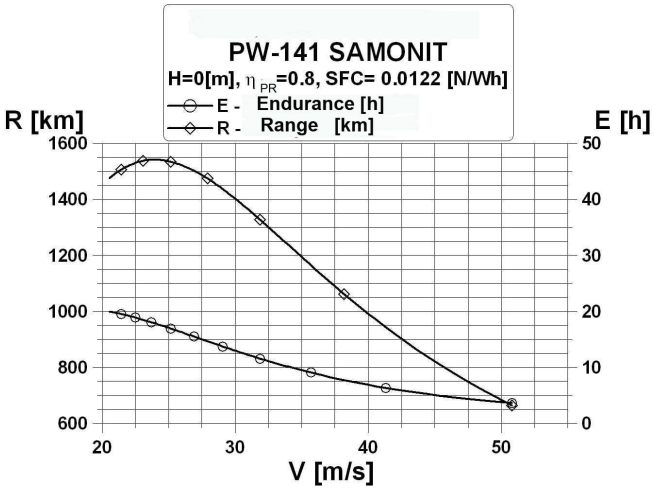

Fig. 29 Range and endurance of tailless configuration, fixed-pitch propeller at its maximum efficiency = 0.8

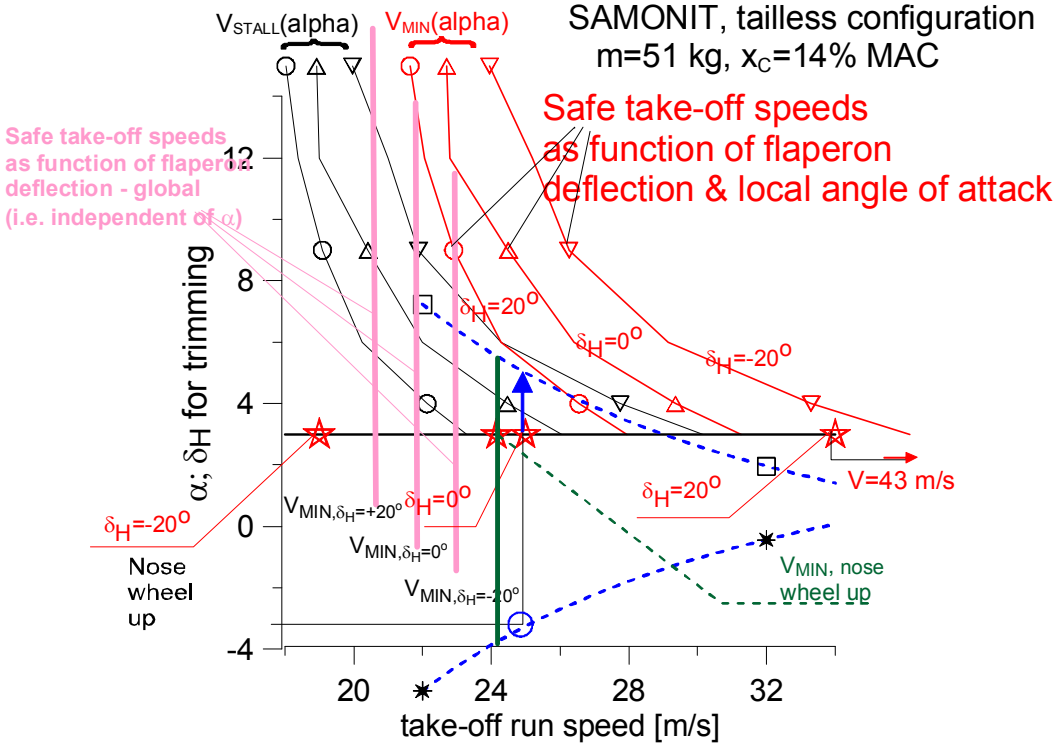

Fig. 30 Different take-off scenarios for tailless configuration. Green colour marks the trimming condition ensuring a safe speed margin for take-off

References

[1] Goraj Z. Civilian Unmanned Aerial Vehicles – Overview of European Effort and Challenges for the Future. Aviation Journal, Vilnius 2003, Aviation, Vol.VII, No 2, pp.1-18, 2003.

[2] Goraj Z., Frydrychewicz A. Development Approach of the PW_103 - An Increased Reliability MALE UAV - Under the CAPECON Project Within the V FR of EU. Proc. Of 24th ICAS Congress, Yokohama 2004, Paper 443.

[3] J.Gadomski, B.Hernik, Z.Goraj. Analysis And Opimisation of a Male UAV Loaded Structure. Aircraft Engineering and Aerospace Technology, Vol.78, No. 2, 2006, pp.120-131.

[4] Goraj Z., Frydrychewicz A., de'Tallec C., Hermetz J. HALE UAV platform optimised for a specialized 20-km altitude patrol mission. Proc. Of 24th ICAS Congress, Yokohama 2004, Paper 285.

[5] Goraj Z., Frydrychewicz A., Świtkiewicz R., Hernik B., Gadomski J., Goetzendorf T., Figat M., Suchodolski S., Chajec W. High Altitude Long Endurance Unmanned Aerial Vehicle of a New Generation – a Design Challenge for a Low Cost, Reliable And High Performance Aircraft. Bulletin of Polish Academy of Sciences, Vol.52, No.3/2004, pp.173-194.

[6] Goraj Z. PW-125 MALE UAV design project developed in Warsaw University of Technology. AIAA 3rd conference "Unmanned Unlimitted", Chicago, Sept. 2004, AIAA paper 6326.

[7] Goraj Z.. Design Challenges associated with development of a new generation UAV. Aircraft Engineering and Aerospace Technology, Vol.77, No. 7, 2005, pp.361-368.

[8] Figat M., Goetzendorf-Grabowski T., Goraj Z. Aerodynamic Calculation of Unmanned Aircraft. Aircraft Engineering and Aerospace Technology, Vol.77, No. 6, 2005, pp.467-474.

[9] Schmollgruber P, Gobert J., Gal P., Goraj Z. An Innovative Evaluation platform for New Aircraft Concepts. The Aeronautical Journal, July 2010, Vol.114, No 1157, pp. 451-456.

[10] Goraj Z., Kitmann K., Voit-Nitschmann R., Szender M. Design and Integration of Flexi Bird – a low cost sub-scale research aircraft for safety and environmental issues. 27th ICAS, Nice 2010, p.469.

[11] Goraj Z. An Integrated System for Border Surveillance and Monitoring Based on Very Light MALE UAV. Proc. Of 25th ICAS Congress, Hamburg, Sept 2006, Paper 417.

[12] Goraj Z. UAV platforms designed in WUT for border surveillance. AIAA Infotech @ Aerospace 2007 Conference and Exhibit. San Francisco - Rohnert Park, 7-10 May, 2007.

[13] Goraj Z. Mini UAV Designed for Surveillance Long Endurance Mission. The 4th Internat. Symposium on Innovative Aerial / Space Flyer System. Tokyo, 14 Jan. 2008, Plenary, Invited Lecture. Proc. of the 4th Int. Symposium, pp.11-20.

[14] Galinski Z. Wing section designed for PW-141. SAMONIT internal report, Warsaw, May 2007.

[15] Goraj Z., Chajec W. Aeroelastic Analysis Of Remotely Controlled Research Vehicles With Numerous Control Surfaces. International Journal of Structural Integrity, 2011, Vol.2, No 2, p.158-184.

[16] Goraj Z., Cisowski J., Frydrychewicz A., Grendysa W., Jonas M. Mini UAV design and optimization for long endurance mission. ICAS Congress 2008, USA, Anchorage, paper 437, Sept.2008.

[17] Goraj Z., Frydrychewicz A., Cisowski J., Grendysa W., Jonas M. Progress in design and manufacturing of PW-141 – a long endurance MINI UAS. Seminar of RRDPAE_2008. Paper no 41, Brno, October 2008.

[18] Goraj Z., Nowakowski M, Hajduk J. Long term influence of UAVNET/USICO/CAPECON projects on Polish UAS activities (research / design / testing / production / education etc) , UAVNET Workshop No. 18, Tel Aviv, 20-21 Oct. 2010, www.uavnet.org

[19] Goraj Z. Design, manufacturing and testing of an advanced, tailless, long endurance UAVs – from mini class to MALE design. Proc. of the First International Conference on Unmanned Systems in Israel, AUVSI 2012, Tel Avis, March 20-22, 2012, p.70.

Copyright Statement

This paper contains results of SAMONIT project supported by Polish Ministry of Science and Higher Education, grant no R10/ 010/ 02 under the agreement of 0597/R/2/T02/07/02. Design Team was established under the umbrella of the "Centre of Excellence of Aircraft Design" created at Warsaw University of Technology under the auspices and financial support received from the "Association of Polish Pilots" established in Great Britain, with special acknowledgement addressed to Andrzej Jeziorski - Colonel Pilot and Head of the association.